



## OPEN ACCESS

## EDITED BY

Jan Blahút,  
Institute of Rock Structure and Mechanics  
(ASCR), Czechia

## REVIEWED BY

Mohammad Azarafza,  
University of Tabriz, Iran  
Chun Zhu,  
Hohai University, China

## \*CORRESPONDENCE

Zizhao Zhang,  
✉ zhangzizhao@xju.edu.cn  
Yanyang Zhang,  
✉ zyy@xju.edu.cn

RECEIVED 12 August 2023

ACCEPTED 30 October 2023

PUBLISHED 27 December 2023

## CITATION

Lai R, Zhang Z, Zhang Y, Chen D, Shi G and  
Fu Q (2023), Deterioration mechanism of  
loess from Ili valley region of China under  
wet and dry cycles: evidences from  
shear tests.

*Front. Earth Sci.* 11:1276461.

doi: 10.3389/feart.2023.1276461

## COPYRIGHT

© 2023 Lai, Zhang, Zhang, Chen, Shi and  
Fu. This is an open-access article  
distributed under the terms of the  
[Creative Commons Attribution License  
\(CC BY\)](https://creativecommons.org/licenses/by/4.0/). The use, distribution or  
reproduction in other forums is  
permitted, provided the original author(s)  
and the copyright owner(s) are credited  
and that the original publication in this  
journal is cited, in accordance with  
accepted academic practice. No use,  
distribution or reproduction is permitted  
which does not comply with these terms.

# Deterioration mechanism of loess from Ili valley region of China under wet and dry cycles: evidences from shear tests

Runsen Lai<sup>1</sup>, Zizhao Zhang<sup>1\*</sup>, Yanyang Zhang<sup>1\*</sup>, Debin Chen<sup>2</sup>,  
Guangming Shi<sup>1</sup> and Qiang Fu<sup>3</sup>

<sup>1</sup>School of Geological and Mining Engineering, Xinjiang University, Urumqi, China, <sup>2</sup>The Second Hydrological Engineering Geological Brigade of Xinjiang Bureau of Geology and Mineral Resources, Urumqi, China, <sup>3</sup>Jiangxi Province Survey and Design Research Institute Co., Ltd., Jiangxi Province, China

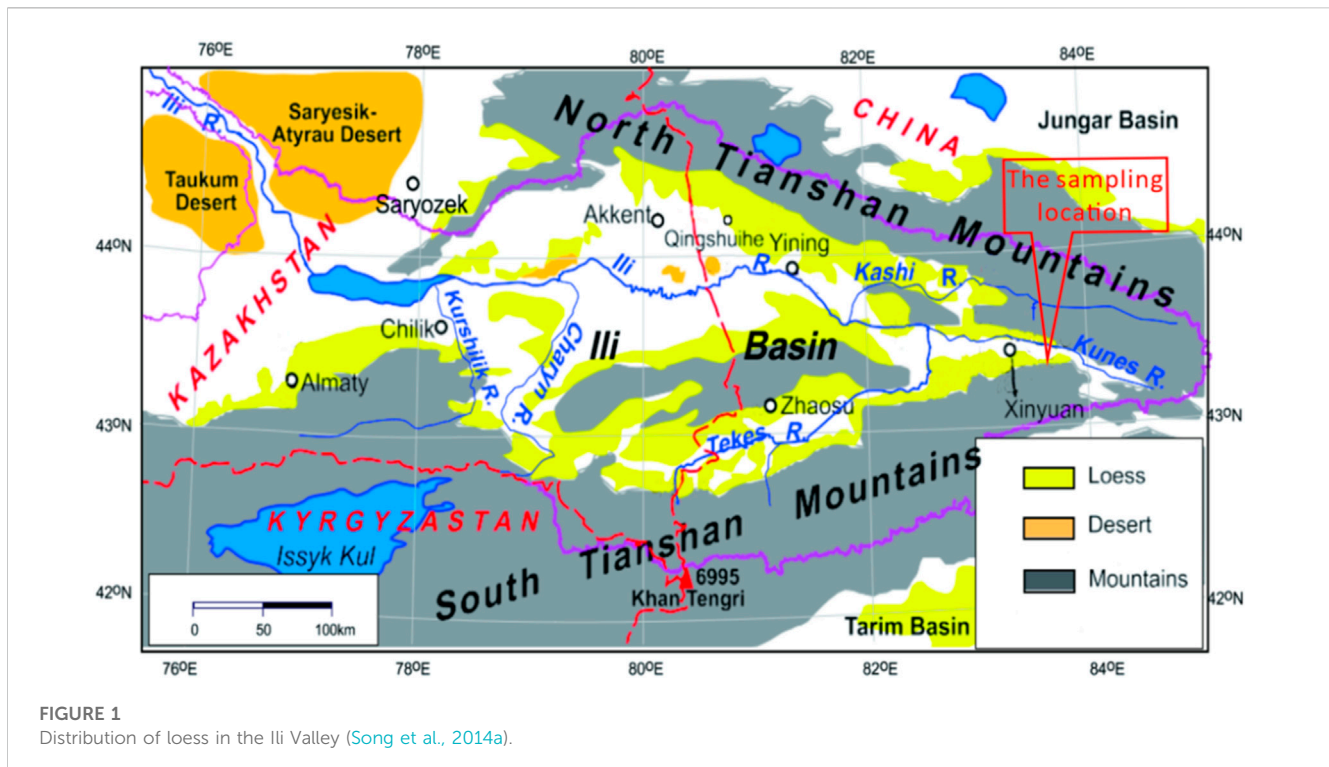
The properties of loess in the Ili region of China are significantly affected by repeated cycles of rainfall and evaporation. It is thus essential to investigate the deterioration mechanism of loess subjected to the wet and dry cycles. This paper employs various methods, including the direct shear and triaxial shear tests, as well as the scanning electron microscopy (SEM), to evaluate the variation patterns of shear strength parameters and microstructure of Ili loess. The direct shear test was conducted on loess samples experiencing a limited number of wet and dry cycles (0, 1, 3, 5, 7, and 9), while the triaxial shear test focused on a more extensive range of wet and dry cycles (0, 1, 3, 10, 20, and 30). In parallel, the alterations in the shear strength parameters of the loess material under different shear tests were also scrutinized. The findings obtained from this research revealed that the shear strength of Ili loess decreased to varying degrees based on the two test methods when they are affected by the wet and dry cycles. Comparing the results with the same number of wet and dry times (0, 1 and 3 times), both the shear strength and cohesion obtained from the triaxial shear test were greater than those from the direct shear test, while the results for the angle of internal friction were reversed. Moreover, the scanning electron microscope tests on Ili loess did indicate that the micro-particle size, pore space, morphology, soil structure, and particle contact mode exhibited the deterioration with different degrees. The micro-structural change is believed to be the main reason for the deterioration mechanism of the shear strength. The research outcomes will enrich the understanding about the loess properties in Central Asia, providing data reference and theoretical basis for engineering construction in these region.

## KEYWORDS

ili loess, drying-wetting cycles, direct shear test, triaxial shear test, microstructure

## 1 Introduction

As a typical structural soil, the water sensitive loess is featured with wet subsidence, disintegration, and dissolution (Feng et al., 2021). The unique properties of the loess result in the distinct differences within variable regions, in particular, when the engineering construction, mechanisms of geological disasters, and the modes of disaster formation are accounted for. It is thus imperative to generalize geological structure models and geomechanical models of loess disasters to reveal the laws governing water-soil



interactions and their disaster-causing mechanisms (Peng et al., 2014). Rainfall-type loess landslides did cause significant economic losses and casualties due to their frequent occurrences and widespread distribution (Li et al., 2022). Examining its formation mechanisms is vital for enhancing the efficacy of geological disaster prevention and control measures in loess regions. A pivotal aspect of such investigations lies in precisely understanding the deterioration law of loess properties and their underlying mechanisms subjected to the wet and dry cycles.

It has been well noted that the widespread geological loess distributed in Asia, Europe, North America, and South America, is particularly abundant in Central Asia, where its substantial thickness, typical deposition patterns, and complete strata are unparalleled globally (Peng et al., 2014). Ili, situated in the Ili Valley at the northern base of the Tianshan Mountains in the central Asian region of the Xinjiang Uygur Autonomous Region, exhibits extensive distribution of loess (Song et al., 2014a) (see Figure 1). This loess primarily corresponds to the Late Pleistocene Malan loess. Compared to the loess in the Loess Plateau, the Ili loess is featured with its coarser grain size, loose structure, and high pore ratio. Consequently, these properties contribute to a greater susceptibility of the loess to moisture and vulnerability (Yin et al., 2009). Attributed to the special geological conditions of Ili region with a large amount of mountainous and river valleys, the abundant rainfall and humidity make it become the most susceptible region with geological disasters in Xinjiang. As one of the 16 critical areas prioritized for geological disaster prevention and control in China, the research either on the formation mechanisms or the disaster-causing factors is essential to prevent geological disasters in the Ili Valley. Note that geological hazards predominantly occur from April to June each year, with over 90% of the total incidents being triggered by rainfall and snowmelt in the Ili Valley. That is, an

in-depth study on the deterioration of loess under the wet and dry cycles is requested.

The wet and dry cycles are believed to be one of the most critical factors deteriorating both the physical and mechanical properties of geotechnical bodies, resulting in the slope instability and structural damage of various engineering foundations. Previous research has successfully demonstrated the influence of wet and dry cycles on loess properties. Primarily, most research focuses on the changes in macro-indicators of physical and mechanical properties and the microstructure of the soil (Tian et al., 2020; Cai et al., 2019; Zhou et al., 2018; Chou et al., 2019). The current research on the loess is primarily on the mechanical strength (Zhou et al., 2018; Chou et al., 2019; Mo et al., 2018; Li et al., 2019; Hu et al., 2020a; Yuan et al., 2017; Qin et al., 2021; Shi et al., 2022; Liu et al., 2022; Yuan et al., 2022; Jian et al., 2020), limited studies were carried out to analyze changes in the microstructure of the soil (Tian et al., 2020; Cai et al., 2019; Ping et al., 2019; Yuan et al., 2022; Jian et al., 2020; Zhang et al., 2022; Nie et al., 2021). Apart from that, there are also some investigations on the influence of mineral content on soil properties (Ping et al., 2019; Hu et al., 2020a; Hu et al., 2020a; Qin et al., 2021; Shi et al., 2022), variations in moisture content (Shi et al., 2022), and alterations in soil-water characteristic curves (Nie et al., 2021; Chou and Wang, 2021). The research methods utilized in these studies encompass in-house tests, notably direct shear tests (Tian et al., 2020; Zhou et al., 2018; Azarafa et al., 2019), triaxial tests (Mo et al., 2018; Li et al., 2019; Hu et al., 2020a; Yuan et al., 2017; Qin et al., 2021), scanning electron microscopy (SEM) (Tian et al., 2020; Mo et al., 2018; Hu et al., 2020a; Nie et al., 2021; Chou and Wang, 2021), nuclear magnetic resonance (NMR) (Yuan et al., 2022), computed tomography (CT scan) (Yuan et al., 2017), and etc.

The mechanical properties deterioration of the loess under dry and wet cycles is mainly manifested on the shear strength of the

geotechnical body. Yuan et al. found that drying-wetting cycles had a deteriorating effect on its shear strength either for the *in situ* loess or the manual compacted loess (Yuan et al., 2017). Ma et al. demonstrated that the drying-wetting cycles diminished the shear strength of the loess, with the pronounced impact on effective cohesion (Ma et al., 2022). Using the conventional triaxial tests, Jian's research identified a decrease in the cohesive strength of the loess under drying-wetting cycles associated with an exponential decay (Xu et al., 2020). Nonetheless, some research demonstrated that the shear strength did not continuously decay with increased number of drying-wetting cycles. A good example is that the shear strength of the compacted loess initially decreased and then gradually increased along with the number of drying-wetting cycles (Wang et al., 2019). The consolidation and drainage triaxial shear tests on the compacted loess revealed that the shear strength of the loess initially decreased and then increased with the number of drying-wetting cycles increasing, reaching a critical point after three to nine cycles (Hao et al., 2021). That is, the deterioration of the loess generally occurred at the beginning of the drying-wetting cycles. However, there are variations in the number of critical times found in the experiments of different researchers. Rui (2018) demonstrated that the first drying-wetting cycle had a more pronounced effect compared to subsequent cycles through suction-controlled direct shear tests. Similarly, the reduction in viscous cohesion was more rapid during the first three drying-wetting cycles, while the decrease slowed down in later cycles. Meanwhile, the internal friction angle remained relatively stable throughout the process (Wang et al., 2021).

Investigation on the deterioration mechanism of soil mechanical properties is always the hot research topic and various factors affecting the behavior of the loess under drying-wetting cycles were evaluated. These critical factors can be primarily categorized into two aspects. The first one is the external factors, including the number of drying-wetting cycles, the magnitude of wet and dry cycles, the lower limit of wet and dry cycles and the temperature. The second aspect involves internal factors, such as moisture content and density. Hu et al. investigated the deterioration of the compacted loess with the consideration of the dry density, drying-wetting cycle amplitude, and lower limit moisture content (Hu et al., 2018; Hu et al., 2020b). Moreover, three factors (i.e., initial moisture content, amplitude of drying-wetting cycles) were taken into consideration (Ye et al., 2020). Pan et al. conducted *in-situ* loess tests with different moisture content and varying numbers of drying-wetting cycles (Pan et al., 2020). Thang et al., 2019 identified four pivotal factors, including pore ratio, net stress, matrix suction, and saturation, which significantly influence the strain shear modulus. Liu et al. investigated the effect of the initial dry density and historical drying stress on drying-wetting cycles (Liu et al., 2014; Liu et al., 2017). Wang et al. concluded that the cutline modulus increases exponentially with initial compaction (Wang et al., 2016). For the variation of shear strength and its study characteristics see Table 1.

The Ili Valley located in the center of Asia is of high vulnerability (A Y S et al., 2014). and the loess in this region exhibits different material compositions and engineering properties, attributed to its unique topography and geological conditions (Liu et al., 2022; Song et al., 2018). Previous research in this region primarily focused on the composition, genesis, and formation environment of the loess. Limited research did concern the changes of loess properties under

the wet and dry cycles (Li et al., 2022; Song et al., 2014a; Qin et al., 2021; Wang et al., 2016). Additionally, either the direct shear or the triaxial shear test was not conducted to simultaneously examine the deterioration mechanism of the loess.

Drawing upon insights from previous research, it has been widely noted that the alternation of wet and dry cycles induces transformations in the micro-composition and structure of loess. These alterations encompass changes in particle size, porosity, water state, and soil particle contact patterns, consequently influencing crucial physical and mechanical properties, such as shear strength, compressive strength, and permeability. In recent years, numerous scholars have compared the formation process of the loess in Ili Valley and the Loess Plateau, either from geological aspect or the mineralogical perspective (Li et al., 2012; Yin et al., 2021; Nikbakht et al., 2022; Xiong et al., 2023). However, the emphasis on the material sources will not directly clarify the deterioration mechanisms of the loess, which governs its physical and mechanical properties under drying-wetting cycles (Zeng and Song, 2013; Ren et al., 2023).

Typical Loess Area Sampling Description: Xinyuan County is located in northwestern China, close to the Central Asia region. Central Asia is famous for its vast loess distribution (Song et al., 2014a), and Xinyuan County, as the border zone between Central Asia and China, has some geographical connectivity and similar natural environment. The loess in this area was mainly formed by wind and hydraulic action during the ice age and interglacial period (Yin et al., 2009), and was affected by similar geological structure, climate and depositional environment in the process of formation. Which makes the soil properties of this loess area similar to those of loess in Central Asia and other areas of China, and the selection of soils from this typical loess area for study can illustrate the changing law of loess properties under the dry and wet effects of loess in Central Asia and other areas of China.

Against the above background, exploring the deterioration mechanism of the Ili loess becomes critical and urgent. Different from previous research, this paper focuses on the loess in the Ili Valley and various methods, including the direct shear test, the triaxial shear test, the scanning electron microscopy (SEM) were simultaneously adopted. The in-depth comparison of the microstructures was carried out to further validate the differences of the loess in the triaxial test and direct shear test. Because that the loess investigated in this research was collected from the centre of region of the Asia, research outcomes obtained from this research can provide reference for engineering construction and slope stability analysis in the regions with similar geological conditions.

## 2 Experimental program

### 2.1 Samples information

The loess used in the present research were collected from a representative loess region close to Xinyuan County, Ili Kazakh Autonomous Prefecture, Xinjiang, China, in Central Asia (Figure 2). Table 2 presents the indicators of the fundamental physical and mechanical properties of the soil. Two distinct test methods were employed to determine the shear strength of loess in the research area. The first one is to conduct a direct shear test utilizing FTDS-1 soil cyclic shear test apparatus, while the other one is to conduct a

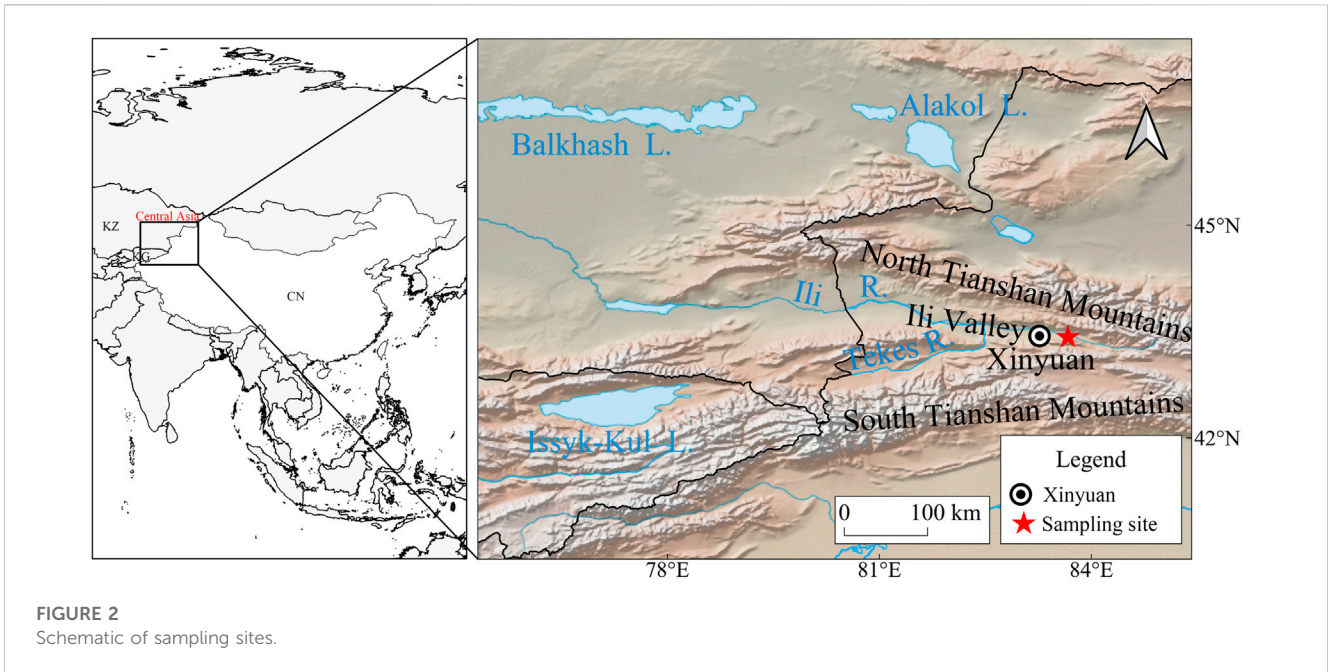


**FIGURE 2**  
Schematic of sampling sites.

**TABLE 1** Summary of changes in shear strength(refer to Poor et al., 2023).

No.	Experimental methods	Factor	Shear strength related changes	Researcher(s)
1	Unconsolidated undrained shear test	<i>In-situ</i> loess and compacted loess	All have a deteriorating effect	Yuan et al. (2017)
2	Triaxial shear tests on unsaturated loesses	Low cycle times (5)	Cohesion is more affected	Ma et al. (2022)
3	Conventional triaxial test	changes in cohesion	exponential decay	Xu et al. (2020)
4	Dynamic triaxial test	compacted loess	decreasing and then gradually increasing	Wang et al. (2022)
5	Solidified drainage triaxial shear test	compacted loess	decrease and then increase, reaching a critical number of cycles under 3–9 wet-dry cycles	Hao et al. (2021)
6	Straight shear test	controlled by suction	the effects of the first wet-dry cycle are more significant	Chen et al. (2018)
7	Straight shear test	different moisture content	Shear strength and wet-dry cycle number of cycles are negatively correlated	Wang et al. (2021)

**TABLE 2** Fundamental physical indicators.

Natural moisture content (%)	Natural density	Natural dry density	Saturated moisture content (%)	Optimum moisture content (%)	Maximum dry density	Porosity ratio	Porosity (%)
20.89	1.96 g/cm <sup>3</sup>	1.64 g/cm <sup>3</sup>	24.57	17.4	1.86g/cm <sup>3</sup>	28.34	22.08

unconsolidated undrained (UU) triaxial shear test using TFB-1 unsaturated soil stress-strain controlled triaxial test apparatus. All these instruments is of the axial force capacity of 30 kN with the measurement accuracy of ±1%. The confining pressures for all samples prepared for the triaxial test were 50 kPa, 100 kPa, and 200 kPa, respectively.

For ease of reference these specimen prepared for the direct shear test is named as Group A and others are referred to Group B. Considering that the loess is a porous, weakly cemented soil with

well-developed vertical joints in engineering practice, (Xie., 2016), the distributions of nodal surfaces and pores within the specimens are much different from each other. Because that the larger-scale specimens offer a better representation of the integrity of the loess and the disparity in strength becomes more pronounced with the increased vertical pressure (Zhu et al., 2020), the 100 mm cubic molds were adopted to cast samples in Group A to simulate larger-sized specimens (Figure 3A), while samples in Group B for conventional shear test is of Φ39.1mm×80.0 mm (Figure 3B). As



listed in Table 2, the moisture content of the samples was 17.4% and the dry density of which was  $1.86 \text{ g/cm}^3$ . After completing a set number of drying-wetting cycles, the specimens were tested and analyzed for changes in the surface morphology of the soil samples using the scanning electron microscopy method (SEM) (Figure 3C).

## 2.2 Drying-wetting cycles

To investigate the wet expansion and dry contraction of loess remodeling samples under cycling wet-dry conditions, an observation test was devised to discern apparent morphological changes. Photographic comparisons were conducted using ring knife samples ( $\Phi 20\text{mm} \times 71.9 \text{ mm}$ ), with particular attention paid to the initial 10 dry and wet cycles. Specimens in Group A were subjected to 0, 1, 3, 5, 7, and 9 cycles. Whereas, specimens in Group B were treated by multiple drying-wetting cycles, encompassing 0, 1, 3, 5, 10, 20, and 30 wet and dry cycles. The drying-wetting cycle process employed the formulated moisture content (17.4%) as the initial moisture content, with a lower limit of 10%. The internal moisture of the soil below the surface does not completely evaporate during natural evaporation, and the soil does not reach a completely dry state and an upper limit of 24.57% (saturated moisture content). One drying-wetting cycle comprises the sequence of initial moisture content-saturated moisture content-lower limit moisture content-and back to the initial moisture content. After undergoing the process of wetting, followed by drying and wetting again until reaching the predetermined moisture content, one drying-wetting cycle is completed for the specimen (Figure 4). The moisture content of the specimen is ensured by controlling the quality of the specimen during the wet and dry cycles.

## 3 Experimental results and analysis

### 3.1 Morphological analysis

During the drying-wetting cycles, the loess remolded specimen exhibited obvious swelling-shrinkage. The morphological changes of the specimens are shown in Figure 5, from which it can be observed that at 0 cycles, the specimen had not undergone. The specimen tightly adhered to the inner wall of the ring knife, and its top was at the same height as the ring knife.

After one cycle, small cracks appeared at the edges of the specimen, however, they were not interconnected in the transverse and longitudinal directions. The surface of the specimen became uneven after wetting. After three cycles, the cracks at the edges of the specimen partially connected in the transverse direction. After five cycles, the cracks at the edges of the specimen fully connected and formed a ring shape along the inner wall of the ring knife, extending towards the center of the specimen and further developing in the longitudinal direction. Several specimens dislodged from the ring, displaying a significantly expanded surface with a granular texture and some soil particles detaching from the lower part of the specimen. After seven cycles, the specimens detached from the ring knife after drying, and there were a few cracks at the center of the specimen. However, the cracks were filled by soil particles, and the surface of the specimen expanded significantly, resulting in the specimen height exceeding the height of the ring knife. After nine cycles, the specimens completely detached from the ring knife, and the gap between the specimen and the ring knife was not filled after wetting. During the drying-wetting cycles, the cracks in the specimens repeatedly closed and opened. With an increasing number of cycles, the quantity, width, and depth of the cracks further increased, severely damaging the connectivity between soil

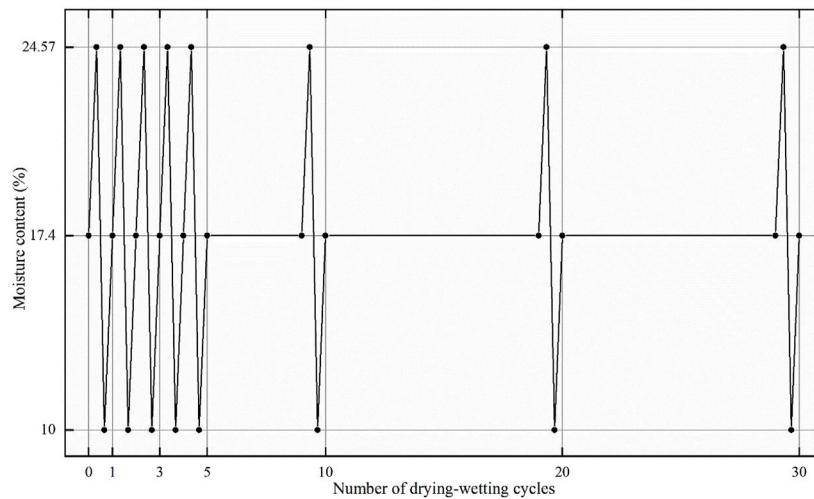


**FIGURE 4**  
Schematic diagram of the drying-wetting cycles process.

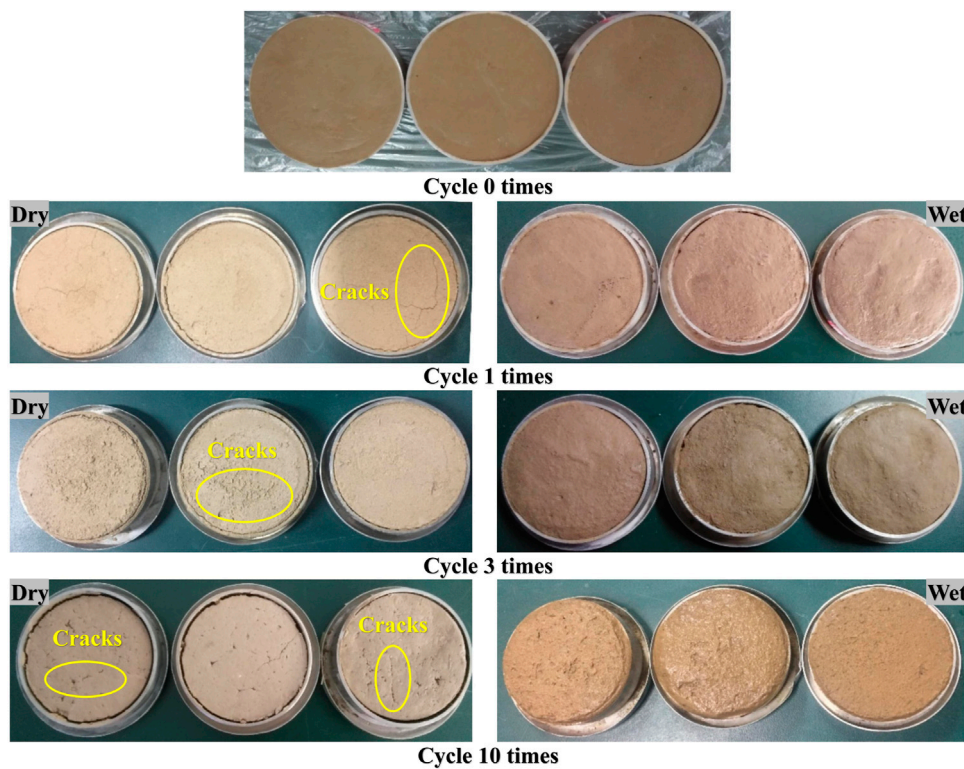


**FIGURE 5**  
Morphological images of some specimens during the drying-wetting cycles (Left is Specimen after drying, whereas, Right is the Specimen after wetting).

particles, leading to a transition of the soil structure from a dense state to a loose state with internal cracks.

From the phenomenon of wet swelling and dry shrinking of loess, it can be concluded that the loess slopes in Asia will undergo certain changes under the effect of alternating cycles of rainfall and evaporation.

During rainfall, loess will absorb water and expand, increasing its volume, making the structure of loess become looser, which will lead to a decrease in the strength of loess slopes and increase the probability of geological disasters; with the gradual evaporation of rainfall, loess gradually loses water, and the phenomenon of drying

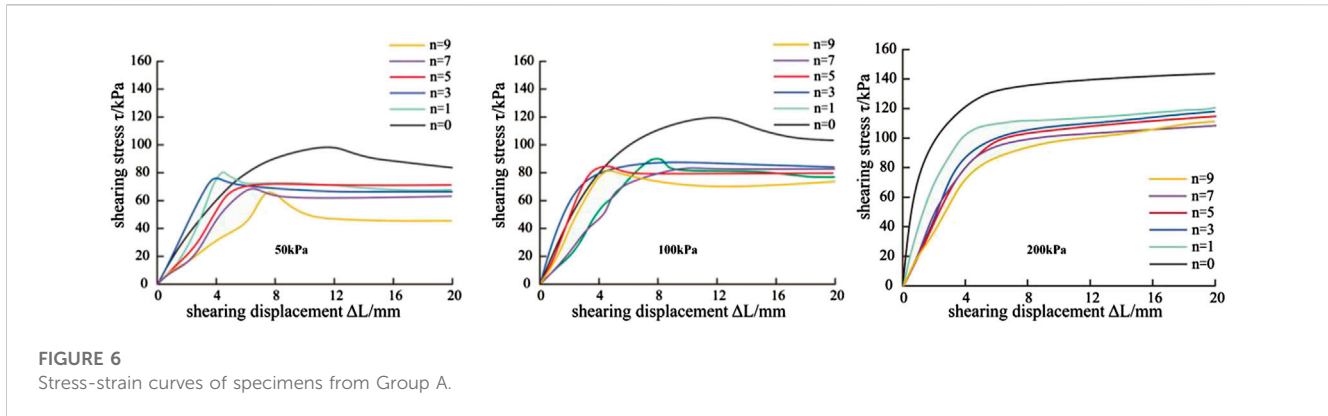


FIGURE 6 Stress-strain curves of specimens from Group A.

TABLE 3 Shear strength and parameters of group A Yili loess under dry-wet cycle.

Cycles numbers	Shear strength ( $\tau_f$ /kPa)			Cohesion ( $c$ /kPa)	Internal friction angle ( $\varphi$ /°)
	$\sigma=50$ kPa	$\sigma=100$ kPa	$\sigma=200$ kPa		
0	98	120	139	88.5	24.30
1	80	89	115	67.0	21.96
3	77	86	113	63.5	22.32
5	72	85	111	59.5	23.40
7	70	84	107	58.5	22.14
9	66	82	105	55.5	22.50

and shrinking occurs, which leads to a decrease in the volume of loess, and the contact between the soil particles becomes closer, thus increasing the stability of the slopes, but it also has the possibility of leading to the formation of loess surface cracks, further increasing the possibility of geological hazards. This shows that the wet-dry cycle has an important influence on the loess properties in Asia.

### 3.2 Variations of strength under the direct shear tests

The specimens from Group A underwent direct shear tests using the FTDS-1 soil cyclic shear test apparatus. The results, as illustrated in Figure 6, demonstrate notable inflection points in shear stress corresponding to different confining pressures. As the number of drying-wetting cycles increases, the position of the inflection points gradually decreases, with the first drying-wetting cycle having the most significant impact on loess strength. By comparing the stress-strain curves under different confining pressures, it can be observed that the curve for the specimens without drying-wetting cycles reaches the highest value. This finding suggests an overall decrease in the shear strength of Group A specimens following the drying-wetting cycles, leading to the deterioration and weakening of their strength.

The results of direct shear test on specimens from Group A were analyzed and the shear strength of specimens under different vertical loads and drying-wetting cycles are listed. The shear strength parameters of the soil in Group A were calculated through fitting the shear strength curve, as shown in Table 3.

Under the influence of drying-wetting cycles, the shear strength exhibited a decrease with an increasing number of cycles at distinct confining pressures, as illustrated in Figure 7. Additionally, the slopes of the curves indicate that the initial drying-wetting cycle has the most notable effect on shear strength. As the number of cycles increases, the influence of a single drying-wetting cycle on soil shear strength diminishes.

### 3.3 Variations of strength under the triaxial shear tests

The data of the triaxial shear test on specimens from Group B were organized to plot the stress-strain curves under different confining pressures. As demonstrated in Figure 8, the specimens at different confining pressures exhibited a peak value of principal stress difference during the shearing process. Compared to specimens that did not suffer from the drying-wetting cycles, those treated specimens experienced a certain reduction in principal stress difference. At 3 and 5 cycles of drying-wetting cycle, there was a slight increase in peak principal stress difference, attributed to changes in the internal structure of the soil, where water pulls soil particles in pore channels and causes pore blockage, leading to soil reinforcement. However, after 10 cycles of drying-wetting, a clear downward trend in peak principal stress difference emerged, similar to the variation pattern observed from specimens of Group A.

By fitting the principal stress with the  $\sigma_1-\sigma_3$  method, the shear strength indicators of Ili loess under different numbers of drying-

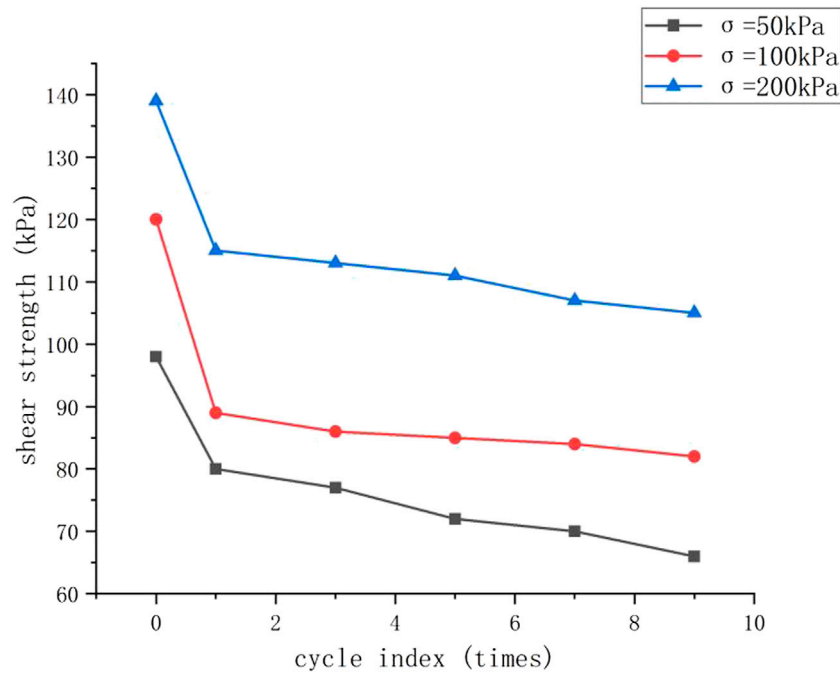


FIGURE 7  
Shear strength variation curve of Group A.

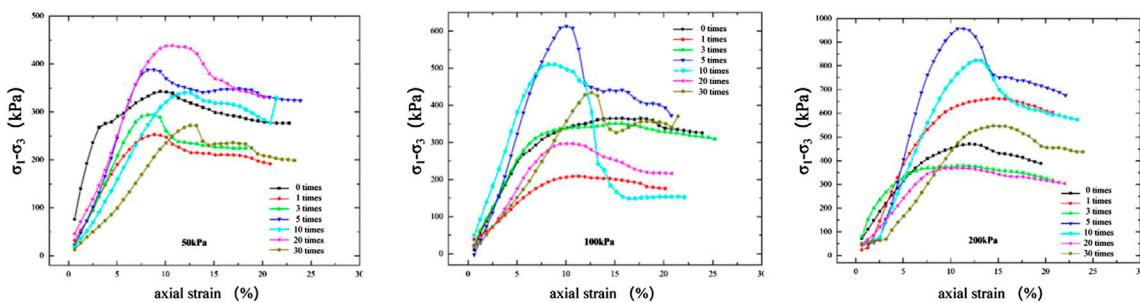


FIGURE 8  
Stress-strain curve of specimens from Group B.

wetting cycles for specimens from Group B were obtained and presented in Table 4. The shear strength of the soil was determined by the Mohr-Coulomb law, considering the shear strength parameters ( $c$ ,  $\phi$ ). The results are presented in Table 3 and Figure 9.

When the specimens were under the wetting-drying cycles, the shear strength of which from Group B decreased significantly, with the most pronounced changes occurring after the initial wetting-drying cycle. However, the shear strength exhibited a slight enhancement and eventually stabilized after fluctuating changes as the number of drying-wetting cycles increased. The final shear strength value was lower than the value before drying-wetting cycles but higher than the value after one drying-wetting cycle.

The comparison of the results of the shear tests in groups A and B shows that the overall reduction of loess shear strength under the action of wet and dry cycles is most pronounced during the initial wet and dry

cycles, and then gradually levels off with the increase in the number of wet and dry cycles, but the overall trend is still decreasing. In the Asian loess region, the alternating cycle of rainfall and evaporation will reduce the shear strength of loess, but this reduction is a gradual process, even if the number of wet and dry cycles increases, the rate of change of shear strength will gradually slow down, which is important for the construction of Asian loess region and the prevention of geological hazards, and need to be considered in the design and construction of loess shear strength changes.

### 3.4 Microstructure evaluation

Scanning electron microscopy experiments were conducted on specimens after different numbers of drying-wetting cycles, and the



TABLE 4 Shear strength and parameters of group B Yili loess under dry-wet cycle.

Cycles numbers (N)	Shear strength ( $\tau$ /kPa)			Cohesion (c/kPa)	Internal friction angle ( $\varphi$ / $^\circ$ )
	$\sigma=50$ kPa	$\sigma=100$ kPa	$\sigma=200$ kPa		
0	229	237	281	81.97	23.16
1	163	181	237	74.34	19.50
3	184	200	209	88.06	17.99
5	182	208	229	81.95	19.70
10	169	202	241	85.09	18.51
20	179	181	224	78.06	19.30
30	182	195	223	88.89	17.81

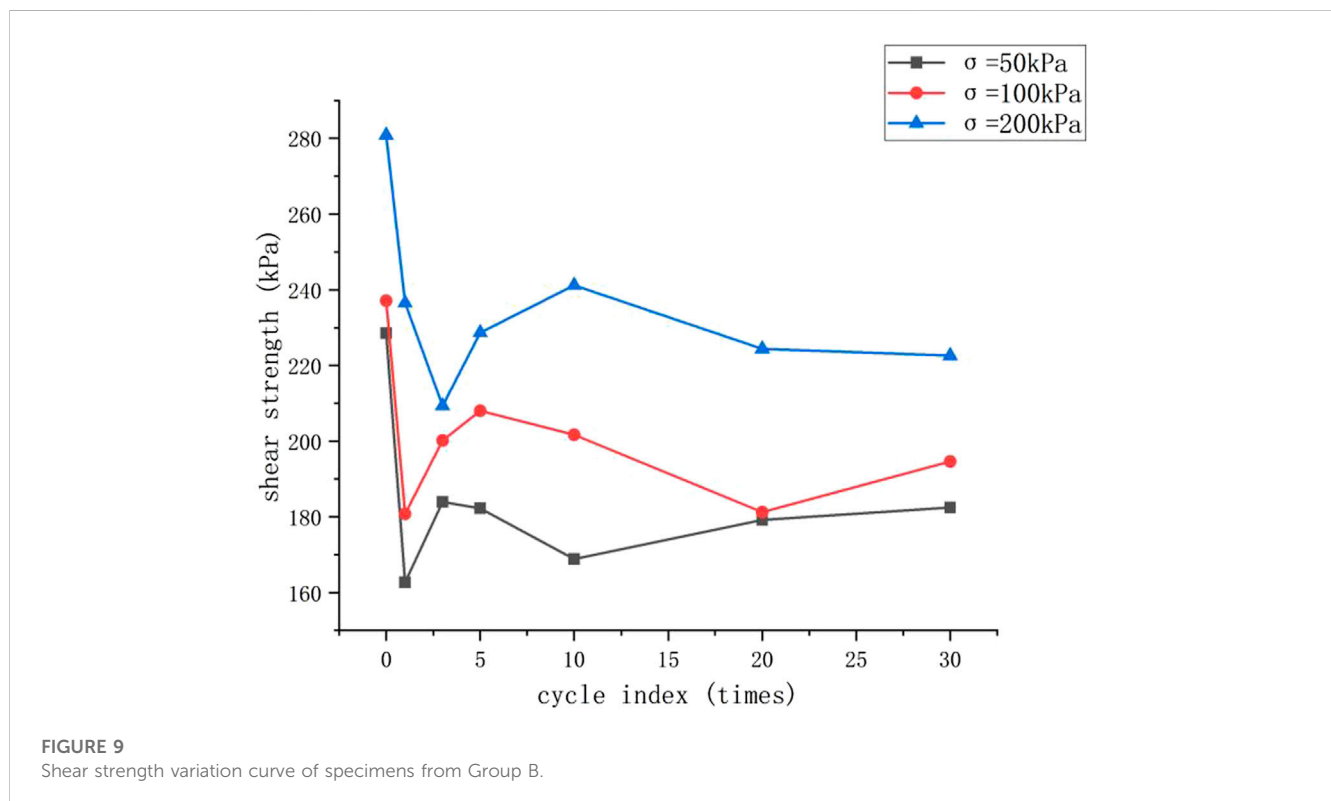


FIGURE 9  
Shear strength variation curve of specimens from Group B.

results of which are presented in Figure 10. In comparison to specimens without any drying-wetting cycles, the loess structure exhibited notable changes under the influence of these cycles. That is, larger particles gradually fractured into smaller ones, and some small particles conglomerated to form aggregates. The soil structure transformed from an initial skeleton structure to an embedded structure. The embedded structure will also be a skeleton structure and finally becomes the flocculated structure. The connectivity between particles changed from face-bonded to contact-bonded, leading to a decrease in shear strength.

To better explore the changes in the microstructure of the soil, quantitative analysis was performed on the size, distribution, shape, and oriented arrangement of soil particles as well as the pores distribution. Characteristic parameters of soil particles or pores were statistically

analyzed to obtain the variation pattern of the microstructure under drying-wetting cycles. The selected microstructural parameters including the average diameter, abundance, and anisotropy ratio (Ye et al., 2020) are illustrated in Figure 11.

It can be observed from Figure 11 that all microstructural parameters of the soil exhibited the change under the influence of wetting-drying cycles. The fluctuation of the average pore size was relatively significant, and it decreased compared to specimens without drying-wetting cycles. This finding indicates that the wetting-drying cycles led to an overall reduction in soil pore size. Abundance reflects the shape of particle units or pores, and it increased overall under the influence of wetting-drying cycles, suggesting that the degree of circularity of particle units or pores increased to some extent. The anisotropy ratio of the soil maintained a decreasing trend after

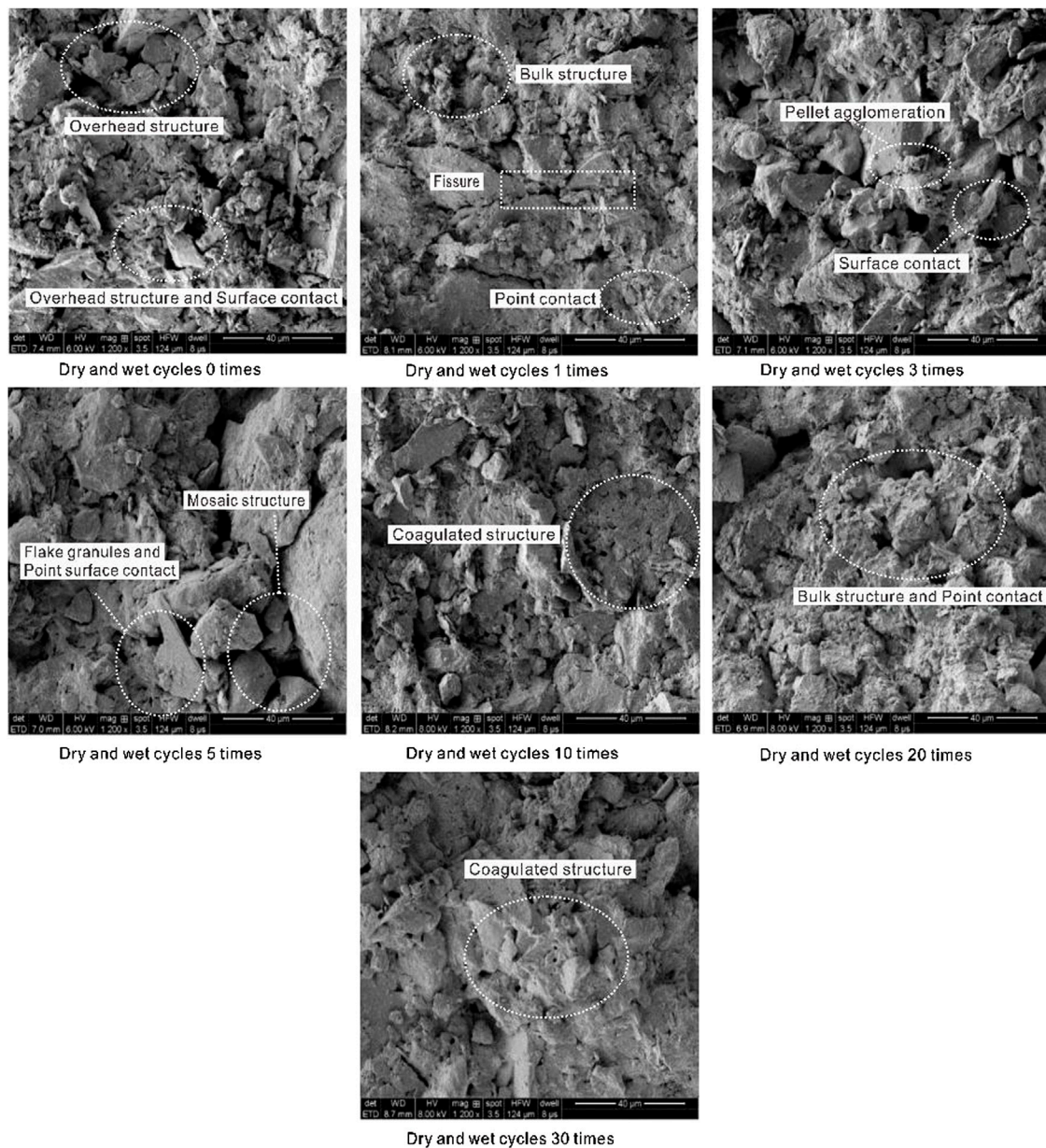


**FIGURE 10**  
Scanning electron microscopy experiments results under different numbers of drying-wetting cycles.

undergoing drying-wetting cycles, indicating that the internal particle units and pores of the soil gradually became more isotropic.

## 4 Discussions

An in-depth comparison among the loess under the direct shear test (Group A) and the triaxial test (Group B) was conducted, when the same number of drying-wetting cycles was given. Note that the shear strength, cohesion ( $c$ ), and internal friction angle ( $\varphi$ ) are depicted in Figures 12–14, respectively. Evidently, the shear strength of the tested specimens acquired from the direct shear test is comparatively lower than that obtained from the triaxial test. Moreover, the shear strength indicators, cohesion ( $c$ ), and internal friction angle ( $\varphi$ ) decrease with an

increased drying-wetting cycles. Furthermore, the cohesion ( $c$ ) obtained from the triaxial test is greater than that from the direct shear test, while the internal friction angle ( $\varphi$ ) from the triaxial test is smaller than that from the direct shear test.

Because that the cubic specimen used for the direct shear test is larger than that adopted in the triaxial test, the larger specimens may contain more joint surfaces and pores, leading to a lower shear strength of the loess. Moreover, the confining pressure applied on the specimens and the strictly controlled drainage may result in a well-distributed stress distribution for the triaxial shear test. The fixed shear plane for the direct shear test gradually decreased and led to an overall lower shear strength, when it is compared with that from the triaxial test. Additionally, the cohesion of Group A is smaller than that of Group B because that the

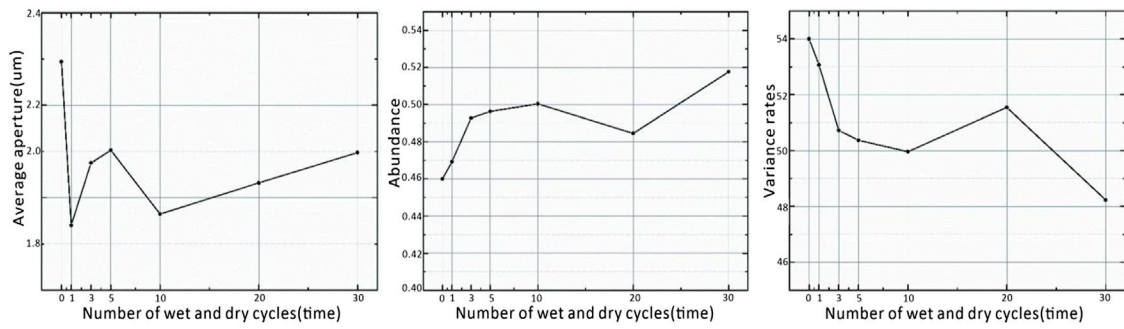


FIGURE 11

Relationship between the numbers of drying-wetting cycles and microstructural parameters.

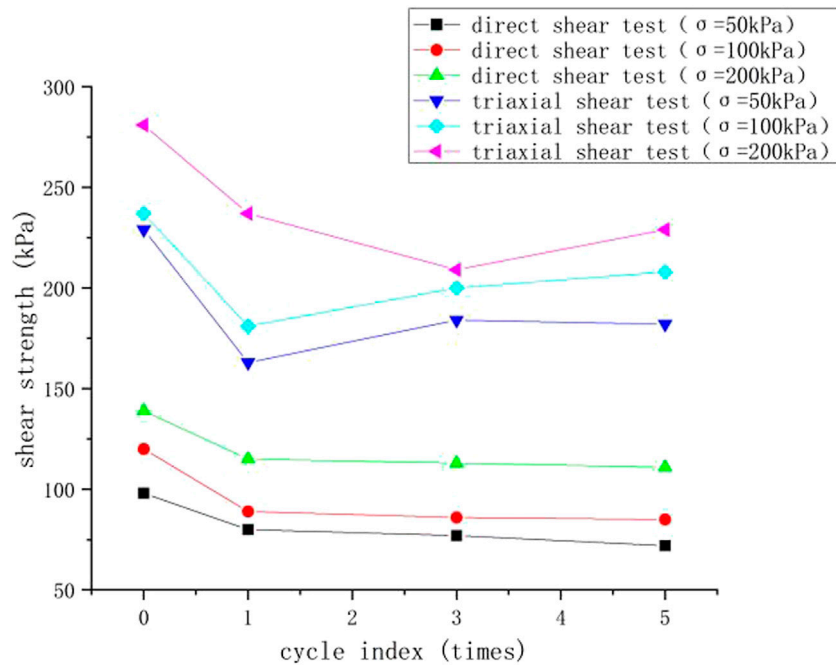


FIGURE 12

Comparison of shear strength.

direction of the principal stress changes continuously during the direct shear test, leading to uneven stress distribution on the shear plane and the shear plane not being the weakest plane. These reasons also explain why the internal friction angle of Group A is greater than that of Group B. The above discussion further confirmed the fundamental and principle differences between the two test methods (Xu., 2012).

Different from previous research (Chou et al., 2019; Ping et al., 2019; Hu et al., 2020a; Yuan et al., 2017; Qin et al., 2021; Liu et al., 2022; Jian et al., 2020; Ma et al., 2022), the internal friction angle exhibits a consistent decrease in all observed cases, except after five cycles, while the cohesion displays fluctuations with the increasing number of drying-wetting cycles. It should be noted that the internal friction angle reflects the size of the frictional force between the loess particles

resisting deformation, including sliding and interlocking friction. In practice, the loess exhibits a large internal friction angle due to the irregularity of soil particles. With the continuous undergoing of the drying-wetting cycles, larger particles will fracture into smaller ones (Figure 12), and the frictional force between loess particles transitions from interlocking friction to sliding friction. Consequently, the internal friction angle of the soil undergoes a certain extent of reduction under the influence of drying-wetting cycles.

The soil structure undergoes changes under drying-wetting cycles (Figure 10), which transits from a skeletal structure to an embedded structure, followed by a granular structure and the flocculated structure (Liu et al., 2022). Under the influence of the fifth drying-wetting cycles, the shape coefficient of soil particles reaches its lowest value with flake-like edges associated with the embedded structure (see Figure 11). It

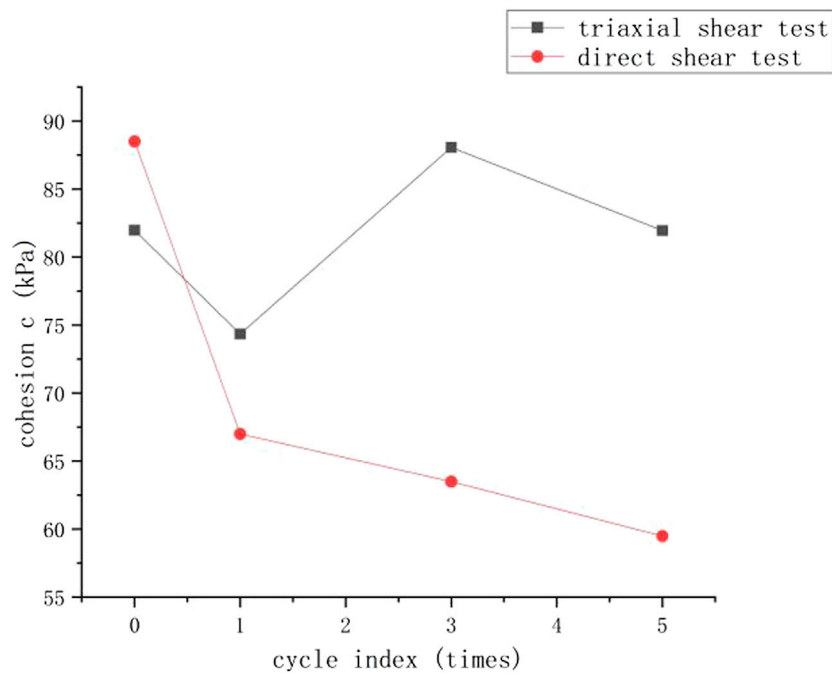


**FIGURE 13**  
Comparison of cohesion.

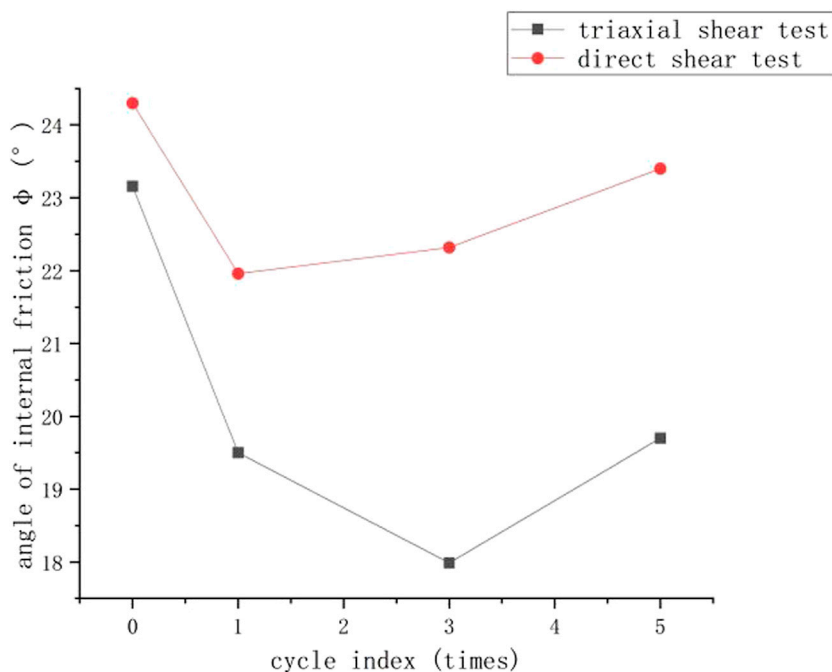


**FIGURE 14**  
Comparison of internal friction angle.

may result in a stronger interlocking friction, leading to an increase in the internal friction angle. The fluctuation in cohesion is mainly related to the contact mode between particles and the status of fine particles (Wang et al., 2021; Ye et al., 2020). When the contact between particles

is of face-to-face, fine particles are within a cohesive state attributed by the relatively high cohesion. Whereas, if the contact of particles is in the form of the point-to-point or point-to-face, fine particles will be within the loose state and the cohesion will be relatively low.

According to the research of the two scholars (Yuan et al., 2017; Mu et al., 2018), the shear strength of the loess obtained from the direct shear test was smaller than that of the triaxial test, when the enclosing pressure was 100 kPa, 200 kPa, and 300 kPa, respectively. To better verify the above observation, the referred data of the loess from the Shaanxi Province of China with the same number of wet and dry cycles (0, 1, 3 and 6) was compared herein. It can be seen from these two research results that the shear strength of the loess obtained from the triaxial shear test is greater than that of the direct shear test, which agrees well with previous discussions.

The direct shear test primarily focuses on the impact of a low number of dry and wet cycles on loess properties, while the triaxial shear test investigates the effects of multiple cycles of drying and wetting on the same properties. Subsequent studies can consider examining the shear strength of loess using different shear tests under identical numbers of dry and wet cycles. Additionally, further investigations can be conducted on specimens with varying water contents (Tang et al., 2018; Zhu et al., 2021). Moreover, exploring the specimen size effect may benefit from optimization, including the possibility of conducting large-scale direct shear tests, which could enhance the accuracy of loess shear strength parameters. Prevention and control engineering suggestions can be made for loess slopes in the Ili region and Central Asia in general, for example, new constrained concrete arches, constant resistance energy-absorbing anchor cables and prestressed anchor support can be considered (Jiang et al., 2023; Wang et al., 2022; Li et al., 2023) and so on.

## 5 Conclusion

The loess in the Ili region and the central Asia is significantly affected by the repeated alternating cycles of rainfall and evaporation. The deterioration mechanism of the loess was investigated in the present research. Based on the systematic laboratory tests (i.e., the direct shear and triaxial shear tests) and the microstructure analysis, the following conclusions can be drawn:

- 1) The shear strength of the loess generally diminishes throughout the dry and wet cycles, with the most significant alteration observed during the initial drying-wetting cycle. Simultaneously, the internal friction angle demonstrates an overall declining trend, while the cohesion experiences fluctuating changes following the drying-wetting cycles;
- 2) Drying-wetting cycles affects the particle size, morphology, structure, and contact characteristics of the loess, leading to the disintegration of larger particles and the aggregation of smaller particles with homogenous element;
- 3) The structure of the loess shifts from an initially porous arrangement to an embedded structure during drying-wetting cycles, and eventually transforms into a flocculated form;
- 4) The particle contact of the loess changes from primarily face-to-face interaction to the point contact;
- 5) The cohesion of the loess measured from the direct shear test is lower than that obtained from the triaxial shear test. Conversely, the internal friction angle determined from the direct shear test is greater than that obtained from the triaxial shear test.

## Data availability statement

The original contributions presented in the study are included in the article/[Supplementary Material](#), further inquiries can be directed to the corresponding authors.

## Author contributions

RL: Conceptualization, Formal Analysis, Methodology, Validation, Visualization, Writing—original draft. ZZ: Conceptualization, Data curation, Funding acquisition, Project administration, Resources, Supervision, Writing—review and editing. YZ: Conceptualization, Formal Analysis, Investigation, Methodology, Validation, Writing—original draft. DC: Conceptualization, Data curation, Investigation, Writing—original draft. GS: Conceptualization, Formal Analysis, Methodology, Writing—original draft. QF: Conceptualization, Methodology, Writing—original draft.

## Funding

The author(s) declare financial support was received for the research, authorship, and/or publication of this article. This research was funded by the National Natural Science Foundation of China (No. 41967036), Xinjiang Uygur Autonomous Region Special Program for Key R&D Tasks (No. 2021B03004).

## Acknowledgments

Thank teachers and cooperation units for their help.

## Conflict of interest

Author QF was employed by Jiangxi Province Survey and Design Research Institute Co., Ltd.

The remaining authors declare that the research was conducted in the absence of any commercial or financial relationships that could be construed as a potential conflict of interest.

## Publisher's note

All claims expressed in this article are solely those of the authors and do not necessarily represent those of their affiliated organizations, or those of the publisher, the editors and the reviewers. Any product that may be evaluated in this article, or claim that may be made by its manufacturer, is not guaranteed or endorsed by the publisher.

## Supplementary material

The Supplementary Material for this article can be found online at: <https://www.frontiersin.org/articles/10.3389/feart.2023.1276461/full#supplementary-material>

## References

- Azarafza, M., Ghazifard, A., Akgün, H., and Asghari-Kaljahi, E. (2019). Geotechnical characteristics and empirical geo-engineering relations of the South Pars Zone marls, Iran. *Geomechanics Eng* 19 (5), 393–405. doi:10.12989/gae.2019.19.5.393
- Cai, Z. Y., Zhu, X., Huang, Y. H., et al. (2019). Evolution rules of fissures in expansive soils under cyclic action of coupling wetting-drying and freeze-thaw. *Chin. J. Geotechnical Eng.*, 41(08): 1381–1389. doi:10.11779/CJGE201908001
- Chen, R., Xu, T., Lei, W., et al. (2018). Impact of multiple drying–wetting cycles on shear behaviour of an unsaturated compacted clay. *Environ. Earth Sci.* 77, 683. doi:10.1007/s12665-018-7868-6
- Chou, Y., and Wang, L. (2021). Soil-water characteristic curve and permeability coefficient prediction model for unsaturated loess considering freeze-thaw and dry-wet. *Soils Rocks*, 44. doi:10.28927/SR.2021.058320
- Chou, Y. L., Zhang, Q. H., and Jia, S. S. (2019). Experiment on strength of unsaturated remodeled loess based on freeze-thaw and dry-wet effects[J]. *J. Lanzhou Univ. Technol.*, 45(3):8.
- Feng, L., Zhang, M., Jin, Z., et al. (2021). The genesis, development, and evolution of original vertical joints in loess. *Earth Sci. Rev.* 214:103526. doi:10.1016/j.earscirev.2021.103526
- Hao, Y. Z., Wang, T. H., Cheng, L., et al. (2021). Structural constitutive relation of compacted loess considering the effect of drying and wetting cycles[J]. *Rock Soil Mech.*, 42(11):2977–2986. doi:10.16285/j.rsm.2021.0551
- Hu, C. M., Yuan, Y. L., Mei, Y., et al. (2020a). Comprehensive strength deterioration model of compacted loess exposed to drying-wetting cycles[J]. *Bull. Eng. Geol. Environ.*, 79(1):383–398. doi:10.1007/s10064-019-01561-8
- Hu, C. M., Yuan, Y. L., Mei, Y., et al. (2020b). Comprehensive strength deterioration model of compacted loess exposed to drying-wetting cycles. *Bull. Eng. Geol. Environ.* 79, 383–398. doi:10.1007/s10064-019-01561-8
- Hu, C. M., Yuan, Y. L., Wang, X. Y., et al. (2018). Experimental study on strength deterioration model of compacted loess under wetting-drying cycles[J]. *Chin. J. Rock Mech. Eng.*, 37(12):2804–2817. doi:10.13722/j.cnki.jrme.2018.0770
- Jian, Xu., et al. (2020). Damage of saline intact loess after dry-wet and its interpretation based on SEM and NMR. *J. Soils Found.* 60 (4), 911–928. doi:10.1016/j.sandf.2020.06.006
- Jiang, B., Xin, Z., Zhang, X., et al. (2023). Mechanical properties and influence mechanism of confined concrete arches in high-stress tunnels. *Int. J. Min. Sci. Technol.* 2023, 1. doi:10.1016/j.ijmst.2023.03.008
- Li, C. X., Song, Y. G., Wang, L. M., et al. (2012). Distribution age and dust sources of loess in the Ili basin[J]. *Earth Environ.*, 40(3):314–320. doi:10.14050/j.cnki.1672-9250.2012.03.020
- Li, G., Zhu, C., He, M. C., et al. (2023). Intelligent method for parameters optimization of cable in soft rock tunnel base on longitudinal wave velocity. *Tunn. Undergr. Space Technol.* 133, 104905. doi:10.1016/j.tust.2022.104905
- Li, P., Xie, W., Ronald, Y. S., Pak, S., et al. (2019). Microstructural evolution of loess soils from the Loess Plateau of China. *Catena*, 173. 10.006. doi:10.1016/j.catena.2018
- Li, Y. J., Tang, Y. M., Deng, Y. H., et al. (2022). Hazard assessment of shallow loess landslides induced by rainfall: a case study of Luilin County of Shanxi Province. *Chin. J. Geol. Hazard Control*, 33(2):105–114. doi:10.16031/j.cnki.issn.1003-8035.2022.02-13
- Liu, K., et al. (2022). Time-dependence of the mechanical behavior of loess after dry-wet cycles[J]. *Appl. Sci.*, 12(3):1212–1212. doi:10.3390/app12031212
- Liu, W. H., Yang, Q., Sun, X. L., et al. (2017). Influence of drying stress history on the mechanical behaviors of silty clay under saturated condition[J]. *J. Hydraulic Eng.*, 48(2): 203–208. doi:10.13243/j.cnki.slx.20160908
- Liu, W. H., Yang, Q., Tang, X. W., et al. (2014). Mechanical behaviors of soils with different initial dry densities under drying-wetting cycle[J]. *J. Hydraulic Eng.*, 45(3): 261–268. doi:10.13243/j.cnki.slx.2014.03.002
- Liu, Y. Y., Wang, G., Lai, H. P., et al. (2022). Study on macro-micro parameter relationship of undisturbed loess under dry-wet cycle[J]. *J. Hydraulic Eng.*, 53(4): 421–432. doi:10.13243/j.cnki.slx.20210905
- Ma, X. N., Zhang, Y. G., Zhang, P. Y., et al. (2022). Experimental research on the effect of repeated drying-wetting cycles on the mechanical properties of remolded unsaturated loess. *Railw. Eng. Soc.*, 39(01):1–6+12.
- Mo, T. F., Guo, M. X., Lou, Z. K., et al. (2018). The effect of moisture content on deformation and shearing characteristics of Ili loess[J]. *China Rural Water Hydropower*, 2018(04):87–90+94.
- Mu, H., Deng, Y., and Li, R. (2018). Experimental study on strength characteristics of loess at ground fissures in xi'an under action of dry and wet cycle. *J. Eng. Geol.* 26 (5), 1131–1138. doi:10.13544/j.cnki.jeg.2018022
- Ni, W. K., Yuan, Z. H., Tang, C., et al. (2017). Experimental study of structure strength and strength attenuation of loess under wetting-drying cycle[J]. *Rock Soil Mech.*, 38(7): 1894–1902. doi:10.16285/j.rsm.2017.07.007
- Nie, Y., et al. (2021). The influence of drying-wetting cycles on the suction stress of compacted loess and the associated microscopic mechanism[J]. *Water*, 13(13): 1809–1809. doi:10.3390/w13131809
- Nikbakht, M., Sarand, F. B., Esmatkah Irani, A., Hajjalilue Bonab, M., Azarafza, M., and Derakhshani, R. (2022). An experimental study for swelling Effect on repairing of cracks in fine-grained clayey soils. *Appl. Sci.* 12 (17), 8596. doi:10.3390/app12178596
- Pan, Z., Yang, G., Ye, W., et al. (2020). Study on mechanical properties and microscopic damage of undisturbed loess under dry and wet cycles. *J. Eng. Geol.* 28 (6), 1192. doi:10.13544/j.cnki.jeg.2019-423
- Peng, J. B., Lin, H. C., Wang, Q. Y., et al. (2014). The critical issues and creative concepts in mitigation research of loess geological hazards[J]. *J. Eng. Geol.*, 22(4): 684–691. doi:10.13544/j.cnki.jeg.2014.04.014
- Pham Ngoc, T., Fatahi, B., and Khabbaz, H. (2019). Impacts of drying-wetting and loading-unloading cycles on small strain shear modulus of unsaturated soils. *Int. J. Geomechanics*, 19. doi:10.1061/(ASCE)GM.1943-5622.0001463
- Poor, M. M., Azarafza, M., and Derakhshani, R. (2023). A correlation based on pressuremeter, SPT and CPT tests for characterizing of coastal alluvium: a study for phase 14 South Pars, Iran. *MethodsX* 10, 101938. doi:10.1016/j.mex.2022.101938
- Ping, Li., Wanli, Xie., Ronald Y. S., Pak., et al. (2019). Microstructural evolution of loess soils from the Loess Plateau of China. *J. catena*. 173. doi:10.1016/j.catena.2018.10.006
- Qin, Y., Li, G., Chen, X., et al. (2021). Study on shear strength and structure of Malan loess under wetting-drying cycles. *Arabian J. Geosciences*, 14. doi:10.1007/s12517-021-09259-6
- Ren, F. Q., Zhu, C., He, M. C., Shang, J. L., Feng, G. L., and Bai, J. W. (2023). Characteristics and precursor of static and dynamic triggered rockburst: insight from multifractal. *Rock Mech. Rock Eng.* 56 (3), 1945–1967. doi:10.1007/s00603-022-03173-3
- Shi, G., et al. (2022). Effect of mica content on shear strength of the Yili loess under the dry-wet cycling condition[J]. *Sustainability*, 14(15):9569–9569. doi:10.3390/su14159569
- Song, Y., Chen, X., Qian, L., et al. (2014a). Distribution and composition of loess sediments in the Ili basin, central Asia [J]. *Quat. Int.*, 334-335:61–73. doi:10.1016/j.quaint.2013.12.053
- Song, Y., et al. (2018). Abrupt climatic events recorded by the Ili loess during the last glaciation in Central Asia: evidence from grain-size and minerals[J]. *Asian Earth Sci.*, 155:58–67. doi:10.1016/j.jseae.2017.10.040
- Tang, S. B. (2018). The effects of water on the strength of black sandstone in a brittle regime. *Eng. Geol.* 239, 167–168. doi:10.1016/j.enggeo.2018.03.025
- Tang, S. B., Yu, C. Y., Heap, M. J., Chen, P. Z., and Ren, Y. G. (2018). The influence of water saturation on the short- and long-term mechanical behavior of red sandstone. *Rock Mech. Rock Eng.* 51 (9), 2669–2687. doi:10.1007/s00603-018-1492-3
- Thang Pham, Ngoc., Behzad, Fatahi., and Hadi, Khabbaz. (2019). Impacts of Drying-Wetting and Loading-Unloading Cycles on Small Strain Shear Modulus of Unsaturated Soils. *Int. J. Geomech.* 19 (8). doi:10.1061/(ASCE)GM.1943-5622.0001463
- Tian, H., Li, L., Zhang, K., et al. (2020). Effects of dry-wet and freeze-thaw cycles on microstructure of soil based on SEM. *J. Lanzhou Univ. Technol.*, 46(4):6.
- Wang, F., Li, G. Y., Mu, Y. H., et al. (2016). Experimental study of deformation characteristics of compacted loess subjected to drying-wetting cycle. *Rock Soil Mech.*, 37(8): 2306–2312. doi:10.16285/j.rsm.2016.08.024
- Wang, H., Cao, Y., Ren, J., et al. (2021). Analysis of strength characteristics of expansive soil modified with silty sand under dry-wet cycle[J]. *Sci. Technol. Eng.*, 21(26): 11336–11342.
- Wang, Qi, Xu, S., Xin, Z., et al. (2022). Mechanical properties and field application of constant resistance energy-absorbing anchor cable. *Tunn. Undergr. Space Technol.* 125, 104526. doi:10.1016/j.tust.2022.104526
- Wang, T. H., Hao, Y. Z., Wang, Z., et al. (2019). Experimental study on dynamic strength properties of compacted loess under wetting-drying cycles[J]. *Chin. J. Rock Mech. Eng.*, 39(6):1242–1251. doi:10.13722/j.cnki.jrme.2019.0945
- Xie, D. Y. (2016). *Loess soil mechanics*. 1 edition. Beijing: Higher Education Press.
- Xiong, F., Zhu, C., Feng, G., Zheng, J., and Sun, H. (2023). A three-dimensional coupled thermo-hydro model for geothermal development in discrete fracture networks of hot dry rock reservoirs. *Gondwana Res.* 122, 331–347. doi:10.1016/j.gr.2022.12.002
- Xu, J., et al. (2020). Damage of saline intact loess after dry-wet and its interpretation based on SEM and NMR[J]. *Soils Found.*, 60(4):911–928. doi:10.1016/j.sandf.2020.06.006
- Xu, J., Li, Y., Wang, S., et al. (2022). Shear strength and mesoscopic character of undisturbed loess with sodium sulfate after dry-wet cycling. *Bull. Eng. Geol. Environ.* 79, 1523–1541. doi:10.1007/s10064-019-01646-4
- Xu, Z. (2012). Direct shear test and triaxial shear test comparison analysis [C]. Architecture Technology and Management' Organizing Committee. *Archit. Technol. Manag. Symposium Proc.* 2012:26–27.

- Ye, W., Bai, Y., Cui, C., et al. (2020). Deterioration of the internal structure of loess under dry-wet cycles. *Adv. Civ. Eng.*, 2020: 1–17. doi:10.1155/2020/8881423
- Ye, W., Qiang, Y., Zhang, W., et al. (2020). Macroscopic and microscopic experimental study on remolded loess under humidification-de-humidification conditions[J]. *Sci. Technol. Eng.*, 20(29):12058–12064.
- Yin, G. H., Wang, L. M., Yuan, Z. X., et al. (2009). Physical index, dynamic property and landslide of Ili loess. *Arid. Land Geogr.* 32, 899–905. doi:10.13826/j.cnki.cn65-1103/x.2009.06.018
- Yin, Q., Wu, J. Y., Zhu, C., He, M. C., Meng, Q. X., and Jing, H. W. (2021). Shear mechanical responses of sandstone exposed to high temperature under constant normal stiffness boundary conditions. *Geomechanics Geophys. Geo-Energy Geo-Resources* 7, 35. doi:10.1007/s40948-021-00234-9
- Yuan, K., Ni, W., Lü, X., et al. (2022). Influence of wetting–drying cycles on the compression behavior of a compacted loess from microstructure analysis. *Bull. Eng. Geol. Environ.*, 81(9):1–13. doi:10.1007/s10064-022-02854-1
- Yuan, Z. H., Ni, W. K., Tang, C., et al. (2017). Experimental study of structure strength and strength attenuation of loess under wetting-drying cycle. *Yantu Lixue/Rock Soil Mech.*, 38(7):1894–1902 .
- Yue, Li., et al. (2018). New evidence for the provenance and formation of loess deposits in the Ili river basin, arid central Asia. *Aeolian Res.*, 35:1–8.
- Zeng, M. X., and Song, Y. G. (2013). Mineral composition and their weathering significance of zhaosu loess-paleosol sequence in the Ili basin, Xinjiang. *Geol. Rev.*, 59(03):575–586. doi:10.16509/j.georeview.2013.03.020
- Zhang, W., Li, Y., Wang, R., et al. (2022). A model for the formation and evolution of structure of initial loess deposits. *Catena*, 214. doi:10.1016/j.catena.2022.106273
- Zhou, Y. L., Wu, X. P., Li, F., et al. (2018). Experimental study on influence of freeze thaw cycles and dry-wet alternation on mechanical properties of loess. *Railw. Eng.*, 58(4):4. doi:10.3969/j.issn.1003-1995.2018.04.24
- Zhu, C., He, M. C., Jiang, B., Qin, X. Z., Yin, Q., and Zhou, Y. (2021). Numerical investigation on the fatigue failure characteristics of water-bearing sandstone under cyclic loading. *J. Mt. Sci.* 18 (12), 3348–3365. doi:10.1007/s11629-021-6914-0
- Zhu, Y., Jiang, T., Huo, J., et al. (2020). Large scale direct shear test of undisturbed loess in Sanmenxia and its size effect. *J. North China Univ. water Resour. Electr. power(natural Sci. Ed.)*, 41(4):84–89. doi:10.19760/j.ncwu.zk.2020054